Penerbit UTHM

© Universiti Tun Hussein Onn Malaysia Publisher's Office

JAMEA

http://penerbit.uthm.edu.my/ojs/index.php/jamea

e-ISSN: 2716-6201

Journal of Advanced Mechanical Engineering Applications

Methodology in Setting-Up a Three-Dimensional Flow Model for the Strait of Malacca, Malaysia

Ramadhan Ahmed Ramadhan Basiddiq[1], Anas Abdul Rahman[1*], Ayu Abdul-Rahman[2], Azzim Rosli[1], Najwa Syafiqa Marzuki[1], Wan Muhammad Fadhli Arif[1], Syahfiq Misran[1]

[1]Mechanical Engineering Program, Faculty of Mechanical Engineering & Technology, Universiti Malaysia Perlis, Pauh Putra Main Campus, 02600 Perlis, MALAYSIA

[2]Department of Mathematics and Statistics, School of Quantitative Sciences, Universiti Utara Malaysia, 06010 UUM, Sintok, Kedah, MALAYSIA

DOI: https://doi.org/10.30880/jamea.2022.03.02.010
Received 27 September 2022; Accepted 29 November 2022; Available online 13 December 2022

Abstract: As a rapidly developing and expanding country, Malaysia is expected to see an increase in its electricity consumption in the near future. Although known for its abundance of natural resources, specifically petroleum and natural gas, Malaysia has pledged to reduce its dependency on conventional resources and aims to become a carbon-neutral nation by the year 2050. This can be achieved by unlocking sustainable alternatives from the ocean, such as waves and tidal current energy, which are known to be abundant, continuous, and clean. Although various studies had identified several locations along the Straits of Malacca with potential to be used as deployment sites for tidal stream turbines, most of them were focused only on theoretical resource assessment. Since detailed three-dimensional flow models for the Malacca Strait have yet to be thoroughly developed, examined, and discussed, this study aims to provide a preliminary methodology for setting up a three-dimensional numerical model for this region. The analysis of the study consists of three steps: pre-processing using Blue Kenue; processing with Telemac 3D; and post-processing, which visualizes the simulation outcome. The output from the simulation is validated against published measurement data to ensure the accuracy and robustness of the numerical model. The simulation outcome reveals that the southeast part of the Malacca Strait could be a promising area for deploying tidal stream turbines due to the high tidal current velocity in that area. Additionally, it is also observed that the kinetic energy flux increases towards the southeast part of the strait due to the strait's narrow size in that area. Overall, a detailed procedure for setting up a three-dimensional flow model for the Strait of Malacca is presented, and it is hoped that this work could highlight some of the complexity involved in developing an ocean-scale model for this region.

Keywords: Telemac3D, resource assessment, tidal current velocity, marine energy, ocean-scale model, hydrodynamics

1. Introduction

Malaysia is a country experiencing rapid economic growth and development. Hence, a huge amount of power is required to develop the economy. In 2019, the annual energy consumption rose to 175,164 GWh, an increase of around 112 GWh over the preceding two decades [1]. Natural gas, coal, oil, and diesel, as well as other fossil fuels, have been the primary sources of electricity generation in Malaysia. However, these resources are very harmful to the environment, contributing to climate change, affecting people's health, causing oil spills, and also inhibiting photosynthesis in plants [2].

*Corresponding author: anasrahman@unimap.edu.my

Since renewable energy sources do not release carbon dioxide or other greenhouse gases, renewable energy is often mentioned as one of the most effective solutions for mitigating the effects of rising temperatures in almost all debates on climate change. Solar, biomass, municipal waste, mini-hydro, and biogas are among the renewable resources currently in use in Malaysia [3] -[5]. Nonetheless, there is also huge potential to extract energy from the ocean because of its long coastline in the South China Sea and Malacca Strait [4], [6] -[8]. There are three primary sources of ocean energy: tidal, wave, and thermal [9]. Wave energy converters require at least 50 kW/m² of yearly wave power density. However, in Malaysia, the average wave power density is less than 50 kW/m² [7], [10], [11]. Thermal energy might be used in Malaysia in the Sabah region, where the temperature at the bottom depth is around 3°C, while at the surface is 29°C. This temperature difference allows for the employment of ocean thermal energy converters since it is a region with a temperature difference of around 22°C [10]. Nevertheless, the focus of this study is on tidal stream energy since this technology has been extensively researched and examined in European countries but has received little to no attention in Malaysia.

The Malacca Strait is located between Indonesia's Sumatra Island and Peninsular Malaysia, as shown in Fig. 1. The strait is about 805 km long and 25 m deep. The current speed in the strait is around 2 m/s. The current flows from the Pacific Ocean and the South China Sea to the Indian Ocean, which is deeper and located in the northern part of the strait. Because of the constant flow direction of the current, it is evident that there is a potential to extract energy from the strait [12] -[14]. The tide is a natural phenomenon that happens along coastlines. It is the periodic movement of seawater induced by the sun and the moon. In general, tidal currents in deep seas are low, but they may be significantly increased by constrictions and headlands. Therefore, tidal energy is often insufficient to economically sustain power production in most coastal areas. In regions with strong currents, such as between islands, at headlands and entrances to estuaries, it is possible to capture tidal energy [15].

Fig. 1 - Map of the Strait of Malacca from Google maps

1.1 Types of Tides

Tides can be categorised as diurnal, semi-diurnal, or mixed tides. Diurnal tides have a period that corresponds to the moon's complete rotation around the earth (24 hours, 50 minutes). This sort of tide has a daily high tide [16, 17]. On the other hand, semi-diurnal tides have a duration of 12 hours and 25 minutes. This type of tide has a daily cycle of two high tides and two low tides. This semi-daily tidal cycle occurs on most of the globe because these tides would occur on any planet that is not covered by land that prevents the free movement of water [11]. Finally, mixed tides combine the characteristics of diurnal and semi-diurnal tides. When semi-diurnal tides dominate, spring tides have the strongest tidal currents and neap tides have the weakest. When diurnal tides dominate mixed tides, the strongest tidal currents occur at the moon's greatest declination and the weakest at zero declination. Fig. 2 illustrates the tidal height and tidal phases for the three discussed types of tides.

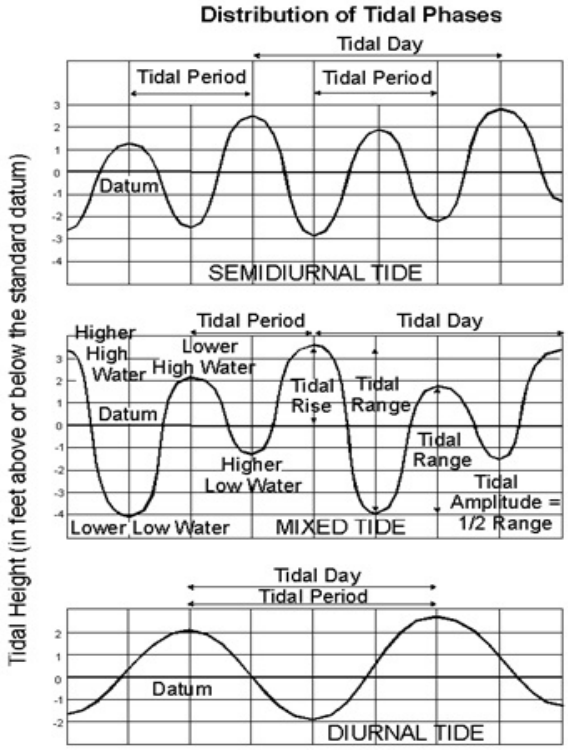

Fig. 2 - Types of tides [18]

1.2 Tides in Malaysia

Malaysia experiences semi-diurnal and mixed tides with dominant semi-diurnal on the west coast of Peninsular Malaysia, while mixed tides with dominant semi-diurnal occur on the east coast, except for Terengganu, where diurnal mixed tides dominate. As shown in Fig. 3, the tide in East Malaysia is mixed with dominant semidiurnal or mixed with diurnal [19].

Fig. 3 - Types of tides as experienced in Malaysia [19]

Tidal energy could be captured mainly in two ways: by utilising the height difference between high and low tides in tidal barriers or the kinetic energy of ocean currents in energy devices, notably tidal current turbines. Even though tidal barrage systems are well-developed and effective, environmental concerns and high construction costs have prevented their widespread expansion. In recent years, this has led to the development of hydrokinetic turbines that capture the kinetic energy in the tidal currents and convert it into electricity [20], as shown in Fig. 4.

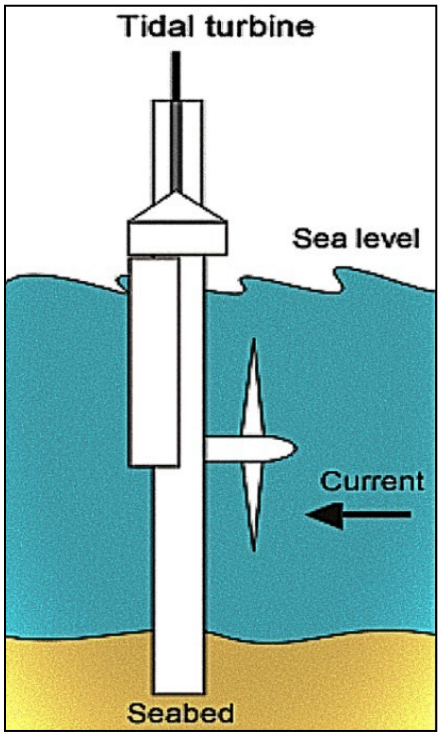

Fig. 4 - Illustration of Tidal stream turbine [20]

There have been several studies discussing the potential of harnessing energy from the ocean in Malaysia. However, many of these studies focused only on the theoretical assessment of resources. For instance, a study conducted by Lee et al. [21] investigated the potential of harnessing tidal energy for electricity generation in Malaysia, although they only examined data such as tidal velocity from the TPXO database. Previously, similar studies by Lee and Seng [22], Sakmani [13], Heap and Wei [23] identified the Malacca Strait as the most promising area for ocean energy extraction due to favourable coastal geometry and grid connectivity. However, details regarding specific sites and their constraints for energy harvesting were not thoroughly discussed. Recent studies by Paul Bonar et al. [12] and Maldar et al. [7] further emphasised the importance of the Strait of Malacca as the main focus area for any ocean energy extraction in Malaysia. Bonar applied an upper bound approach in analysing and determining the maximum power available at potential sites along the west coast of Peninsular Malaysia. However, his depth-averaged model was not able to give details on the current profile along the water column. On the other hand, Maldar et al. [7] mentioned the need for detailed modelling to be conducted to precisely evaluate hydrokinetic resources along the Malacca Strait.

Since detailed three-dimensional flow models for the Malacca Strait have yet to be thoroughly developed, examined, and discussed in the literature, this study aims to provide a preliminary methodology for setting up a three-dimensional numerical model for this region. It is hoped that the methodology presented here can be employed as a reference to develop any ocean-scale models for the Malacca Strait regions by other researchers in the future.

2. Methodology

Numerically assessing the tidal energy convertors installation site requires a dedicated modelling approach that accounts for large-scale oceanic flows over the Malacca Strait and sufficient model resolution in time and space (x, y, z, t). To achieve this, a GeoDAS coastline extractor was used to extract the boundary of the domain, which was acquired online from the National Oceanic and Atmospheric Administration (NOAA) website. The mesh was built after that using Blue Kenue, which consists of regional and high-resolution local mesh. The bathymetry data acquired from GEBCO 2021 were imposed into the mesh and finally, the simulation was conducted using Telemac3D which used the tidal data from TPXO 7.2. Telemac is an effective modelling tool for free-surface flows [24]. After being used in several studies throughout the globe, it became one of the key standards in its industry. The simulation modules use a finite volume scheme in its equations and discretisation methods. Space is discretized using an unstructured grid of triangular elements, allowing it to be refined around regions of interest. The grid/mesh might be generated using the Telemac generator, which is deprecated, or by Blue Kenue software.

2.1 Model Setup

The first step of the hydrodynamic analysis is to define the location of the study area. This study focuses on the Malacca Strait, which has boundaries of 8.4111° North, 102.0212° East, 95.8953° West, and 1.4326° South. Notably, the size of the domain employed is based on the study conducted by Bonar et al. [12]. The location's boundaries were extracted from a high-resolution world map using a GeoDAS coastline extractor. The GeoDAS coastline extractor is a program for analysing, subsetting, and reformatting various shoreline data. Additionally, the software can import and export coasts and borders in various formats. The files that contain the world boundaries and coastlines are available online at the National Oceanic and Atmospheric Administration website (https://www.noaa.gov/).

After extracting the model from the GeoDAS coastline extractor, the model was imported into Blue Kenue. Blue Kenue is an intelligent data preparation, processing, and visualisation software designed for hydraulic modelling. Upon importing the data into Blue Kenue, the boundaries of the domain were edited to ensure stability when performing simulations in Telemac3D. The editing of the boundaries of the domain includes removing very tiny islands, especially the ones close to the coastlines and far away from the area of interest. More importantly, the number of nodes has a significant impact on the generated mesh, since having extremely tiny islands would result in a greater number of unnecessary nodes and elements, hence increasing the simulation's computational time. More often than not, small islands have little influence on the simulation's result; hence, they must either be removed, modified, or merged before the mesh generation.

Notably, editing the boundaries also includes joining some islands that are located very close to one another and removing small water channels. Joining the islands is a crucial step, and the reason for doing so is to avoid problems when generating the mesh, since such small distances between two boundaries often result in critical errors, mainly having over-constrained elements in the mesh when performing the simulations. Similarly, removing small water channels is also essential to avoid having an over-constrained grid generation. Fig. 5 and Fig. 6 highlight the shape of a small part of the domain before and after performing the editing process, respectively. Before the editing was done, countless small islands spread around the gulf, based on the downloaded coastline's geometry from the NOAA website. This is illustrated in Fig. 5, where it can be seen that after editing, the majority of the small islands near Ko Yao Yai and Ko Yao Noi islands had been eliminated from the domain, along with a few little water channels (Fig. 6). Significantly, the two big islands, namely Ko Yao Yai and Ko Yao Noi, were also joined together due to two reasons: (a) The distance between the two islands is very small, approximately 0.037° (i.e., equivalent to 4.107 km) as shown in Fig. 7 (b) These two islands are located far away from the area of interest, which is the Malacca Strait.

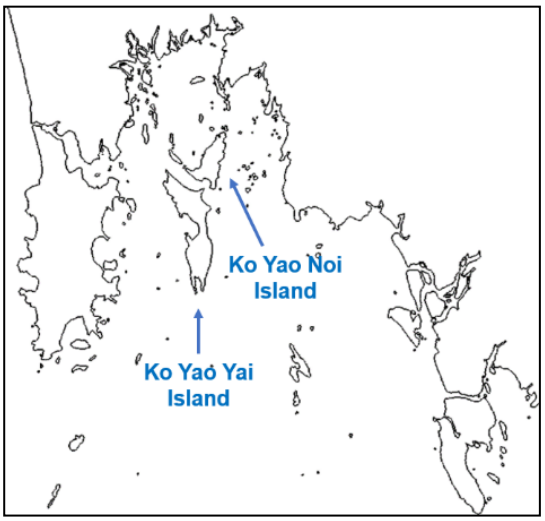

Fig. 5 - Part of the domain BEFORE editing the islands and water channels.

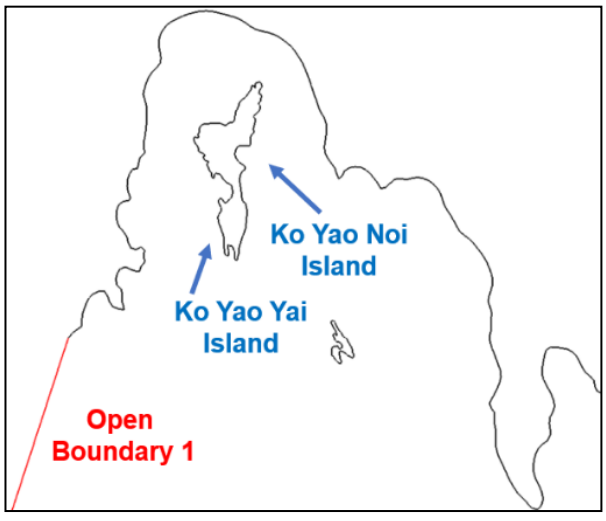

Fig. 6 - Part of the domain AFTER editing the islands and water channels.

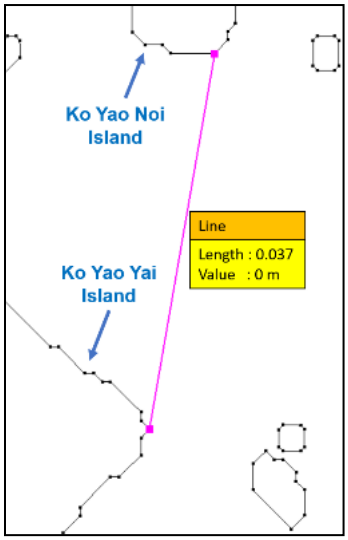

Fig. 7 - Distance between Ko Yao Yai and Ko Yao Noi Islands

2.2 Generating the Ocean Boundaries & Resampling Procedure

To construct a mesh, a fully closed domain is required since a mesh could never be constructed inside an open boundary. Before generating the mesh, the domain of the Malacca Strait must be closed. There are two open boundaries in the Malacca Strait domain, one to the north and the other to the south of the Strait. The two boundaries were closed using Blue Kenue by creating an open line. To have evenly dispersed points along the geometry lines, it is important to resample the geometry lines. The resampling process is the process of rearranging the distribution of the points along the lines of the domain. The resampling process is applied to both the outer boundary of the domain and the boundaries of the islands inside the domain. Fig. 8 shows how the points are unevenly distributed along the boundary of Langkawi Island, while Fig. 9 highlights how the points are distributed along the boundary after performing the resampling process. Caution must be taken in selecting the distance between the points when conducting a resampling exercise of the boundaries. To emphasise, using a higher value for the distance between each node in the domain would alter the shape of the domain significantly.

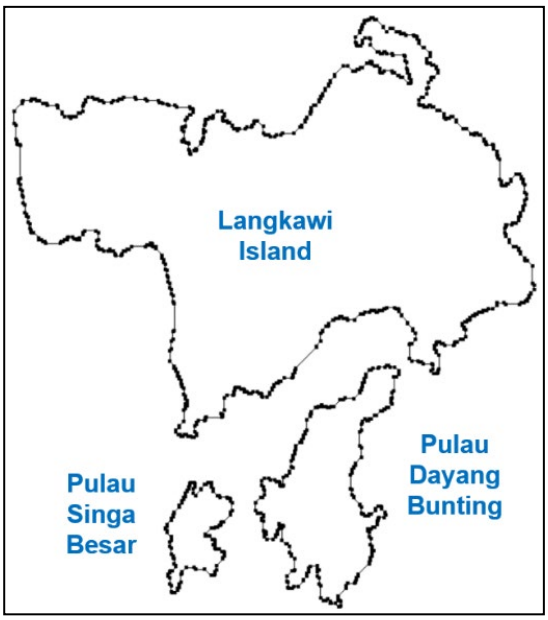

Fig. 8 - Boundary of Langkawi Island before resampling

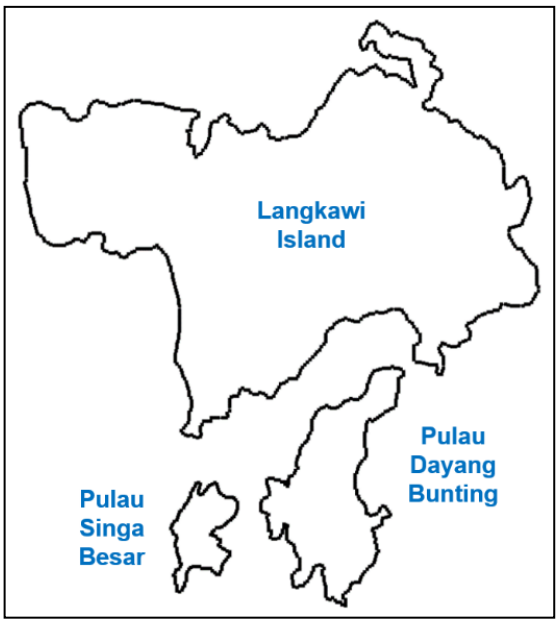

Fig. 9 - Boundary of Langkawi Island after resampling

The method for resampling the coastline differs from the procedure for resampling the islands due to the size difference of the boundaries between the two. The method for resampling the islands allows the user to provide a value that is equal to the number of points along the island boundary plus one point. In contrast, the coastline is resampled by the equal distance method, which is a value entered that corresponds to the distance between each point on the boundary of the coastline. The distance between the points of the coastline was set at 1.11 km.

2.3 Generating the Mesh

The generation of the mesh is a necessity for performing the simulation in Telemac3D. Mesh quality is influenced by several parameters, such as the mesh edge growth ratio and mesh element size. The edge growth ratio defines the maximum distance a mesh element can grow from its neighbour, starting at the boundary. It means that between each segment, the growth of the element connecting two nodes might have a certain ratio to the smallest segment on that node. By default, the mesh element size is the distance between each node along the mesh. In this study, the mesh edge growth ratio chosen is 1.2, meaning that the elements are allowed to grow by 20%. It's important to note that the smaller the value of mesh element size, the greater the number of elements and nodes that would be created along the domain, and vice versa. The same concept also applies to the mesh edge growth ratio.

Fig. 10 illustrates the mesh generated for the domain used in this study for the Malacca Strait. The mesh edge growth ratio used in this domain was 1.2, which is the default mesh edge growth ratio in Blue Kenue software. Additionally, the mesh element size was set to 7.77 km. The resulting mesh, as shown in Fig. 10, has 28,969 nodes and 52,927 elements. This figure also demonstrates the distribution of the elements and nodes along the domain. It is noticeable that throughout the Malacca Strait, where there are no major islands, the mesh's propagation appears to be very smooth. In contrast, as the distribution of the mesh approaches the islands and the coastline, it becomes denser to capture the complex features of the coastline, land masses, and islands.

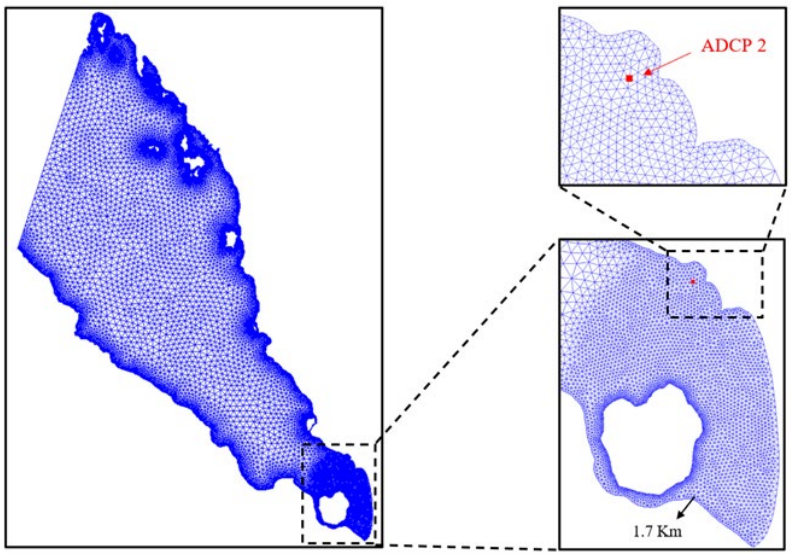

Fig. 10 - The mesh of the Malacca Strait that is used in this study

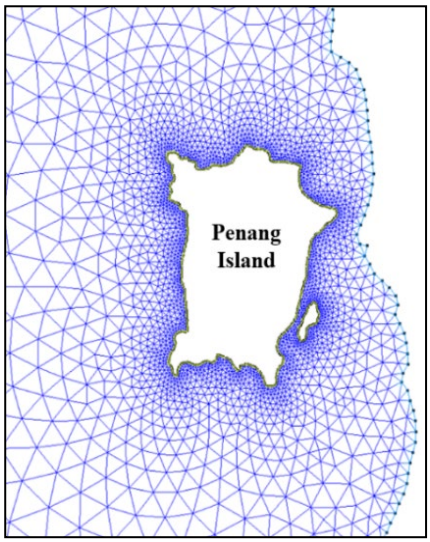

Fig. 11 - Mesh distribution along Penang Island

Similarly, near islands, the mesh becomes more compact to provide a more accurate representation of the island's shape, which was developed and emphasised during the resampling process. A refinement region was added to the mesh at the southeast part of the Strait because that is the area where the validation against the ADCP data is conducted. Hence, the area of interest (i.e., ADCAP points from published data) was imposed with a denser mesh to increase the accuracy of the data to be extracted from those locations. Fig. 11 demonstrates that the distance between the points of the islands is less than the distance between the nodes of the coastline. Due to this reason, the elements appear to be more evenly distributed near the island's boundary lines than along the coastline.

2.4 Imposing the Bathymetry into the Mesh

General Bathymetric Chart of the Oceans (GEBCO) version 2021 was selected in this study to provide data on the depth of the Malacca Strait. The resolution of the 2021 GEBCO is 15 arc seconds, which is approximately 463 m. When choosing the boundaries of the bathymetry data map on the GEBCO website, it is essential to consider the domain of the chosen area of interest. The bathymetry boundaries must extend further than the area of interest bounds, as shown in Fig. 12, where the whole map with the red and orange colours are the boundaries of the GEBCO bathymetry data map while

the domain's boundary is represented with the black lines. After placing the boundaries of the domain on top of the boundaries of the GEBCO data map, the next step was to impose the GEBCO data into the mesh of the domain since the original mesh of the domain had no depth data. Fig. 13 illustrates the mesh of the domain after imposing GEBCO bathymetry data into the mesh.

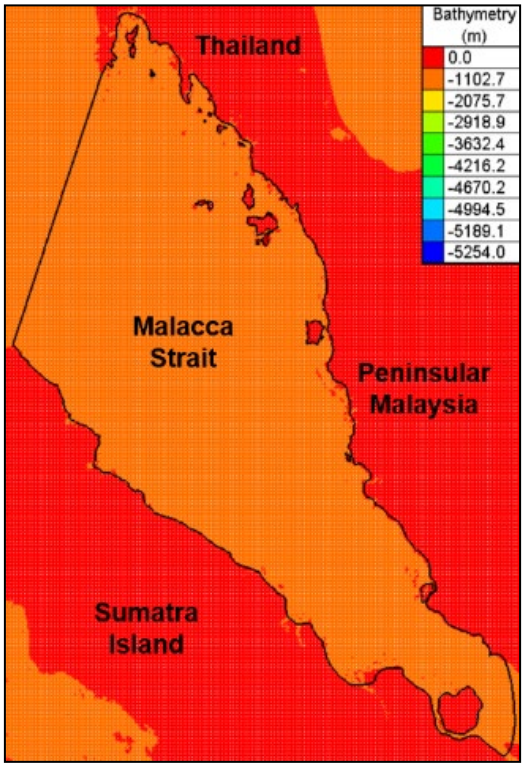

Fig. 12 - Domain map imposed with GEBCO bathymetry map

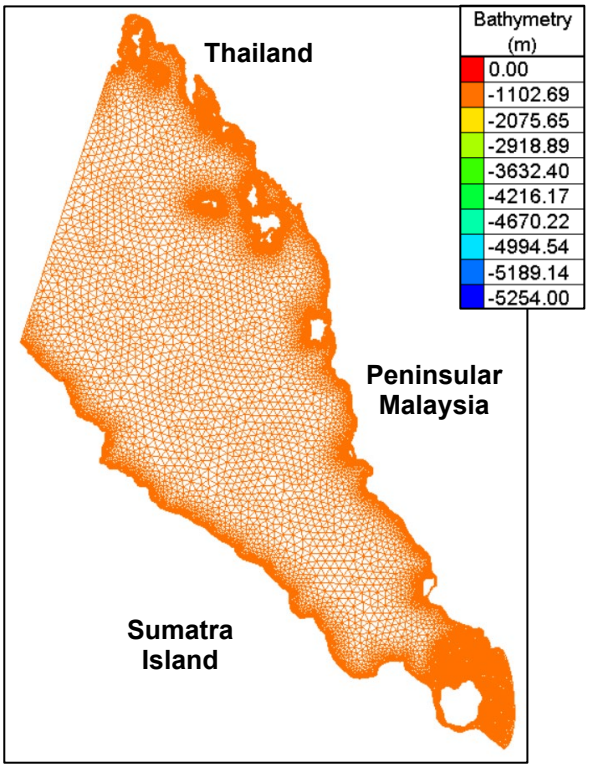

Fig. 13 - Bathymetry of Malacca strait with depth values

The size of the mesh segment or the mesh element size has a significant influence on how the bathymetry data would be imposed on the model. Fig. 14 illustrates the relationship between the generated mesh and bathymetry data. In this figure, the black hexagon denotes a mesh segment with an element length of 1 km that is surrounded by a blue decagon, which represents a bathymetry segment with an element length of 3 km. The three red dots in the figure represent the depth of the ocean within the whole domain. As an illustration, the nodes of the mesh would be able to read the bathymetry data within the mesh segment (i.e., the 1-meter red dot) since the bathymetry segment is bigger than the mesh. In contrast, for the 2 km range that is located between the mesh and the bathymetry segments, the value of the bathymetry will be approximated (i.e., interpolated and extrapolated) by the software. This example explains how the resolution of the bathymetry and the mesh affects the result of the simulation. When the value of bathymetric resolution is smaller than the mesh element size, it could be said that the bathymetry data is highly accurate, and vice versa.

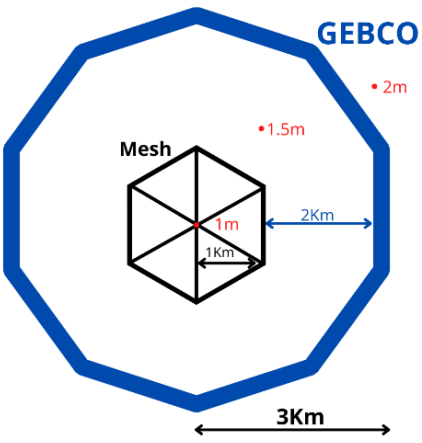

Fig. 14 - Influence of mesh element size on the bathymetry data

2.5 Boundary Conditions & Tidal Data

The tidal data for this study was obtained from TPXO 7.2 (https://www.tpxo.net/tpxo-products-and-registration), which is a series of fully global models of ocean tides. TPXO 7.2's resolution for global tides is 1/4 degree, or 27.75 km. More importantly, the element size of the coastline boundary must be considered, and the distance between each point must be smaller than the element value of TPXO (27.75 km in this study). Otherwise, the resampling process must be repeated with an element value smaller than the TPXO value. The reason for this is to ensure the accuracy of the TPXO data. Otherwise, simulation results would be poor if the element size exceeded TPXO resolution since the model would be required to extrapolate the data to be imposed on the generated domain nodes. This situation is very similar to the one previously discussed regarding the relationship between bathymetry data and mesh resolution (refer to Fig. 14 for clarification).

To apply the tidal data to the created mesh, boundary conditions must be defined. Boundary conditions are predefined areas along the coastline where the tides enter and leave the domain. The boundary conditions have been discussed earlier are denoted as open ocean boundaries, as indicated in Fig. 15. The two boundaries in the domain are the only boundaries that are open for the water current to flow in and out of the domain. The green lines in Fig. 15 represent the liquid open boundary where the flow enters (northern boundary) and leaves (southern boundary) the domain. Meanwhile, the rest of the domain with the brown colour represents a wall (no flow). Notably, the extent of the open boundaries used in this study follows a similar setup as the one outlined by Bonar et al. [12].

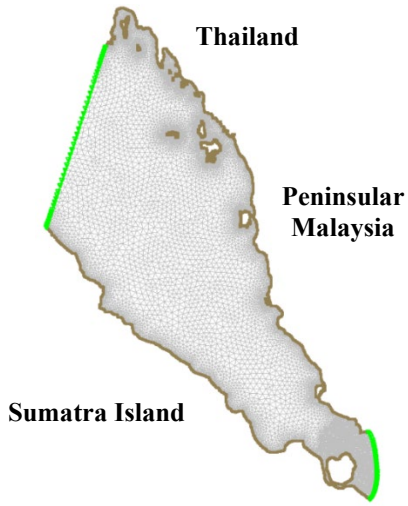

Fig. 15 - The green boundary conditions of the domain

2.6 Numerical Setting for Three-Dimensional Model

The simulation in this study was run using Telemac3D, which is a three-dimensional flow model. Telemac3D solves three-dimensional (3D) equations such as the free surface flow equations (with or without the hydrostatic pressure assumption) and transport-diffusion equations of intrinsic quantities (temperature, salinity, concentration). At each point on the 3D resolution mesh, its main outputs are the velocities in all three directions and the concentrations of transported quantities. Furthermore, it solves the transport of many tracers, which may be classified into two types: "active" tracers, which affect the water density and flow via gravity, and "passive" tracers, which do not impact flow and are just conveyed [25]. Using the following assumptions, the software solves three-dimensional hydrodynamic equations: (a) Three-dimensional Navier-Stokes equations with a time-varying free surface; (b) In the conservation of mass equation (incompressible fluid), the change in density is negligible; (c) The hydrostatic pressure assumption (The pressure at a particular depth is equal to the sum of surface air pressure + weight of the overlying water body); (d) The Boussinesq approximation for momentum (density fluctuations are only considered as buoyant forces). Additionally, Table 1 highlights the numerical settings used in running the 3D models in this study.

Table 1 - Numerical parameters adopted in this study

Parameters	Setting / input
Time Step	2 sec
Simulation Start Date & Simulation Period	12/7/2018 (14 days period)
Initial Condition	TPXO Satellite Altimetry
Number of Horizontal Levels	3 layers
Mesh Transformation	1 (Sigma transformation)

Geographic System & Zone	2 (WGS84 UTM north) Zone 47
Law of Bottom Friction	2 (Chezy Law - default)
Horizontal Turbulence model	3 (k-epsilon)
Vertical Turbulence model	3 (k-epsilon)

2.7 Mesh Edge Growth Ratio

The mesh edge growth ratio is one of the most crucial parameters in mesh generation. In this study, an edge growth ratio of 1.2 was used, which is the default setting. However, in this section, other edge growth ratios are also shown and discussed to demonstrate how the shape of the generated mesh within the domain differs depending on the value employed. Choosing a small value for the edge growth ratio causes the mesh elements to be dense and compact. This is because a smaller ratio value means that the elements can only spread over a very short distance.

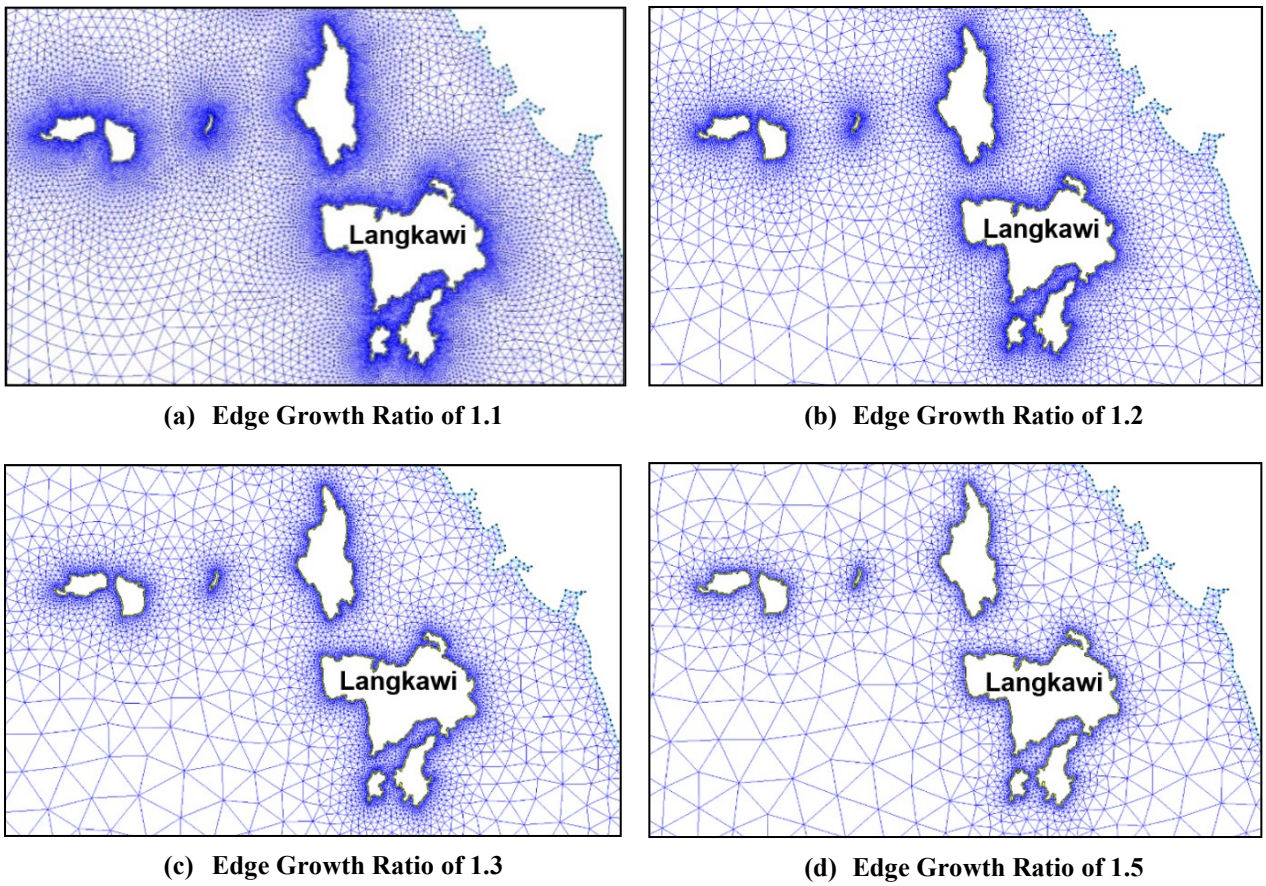

(a) Edge Growth Ratio of 1.1 **(b) Edge Growth Ratio of 1.2**

(c) Edge Growth Ratio of 1.3 **(d) Edge Growth Ratio of 1.5**

Fig. 16 - Mesh generation using four distinct Edge Growth Ratios values

Four meshes were generated with edge growth ratios of 1.1, 1.2, 1.3, and 1.5. The propagation of the four meshes around the island of Langkawi is shown in Fig. 16. The figures show that a mesh with an edge growth ratio of 1.1 results in smaller mesh segments that increase slowly since the elements propagate by 10% from the previous segment. The default mesh ratio, which is 1.2, allows the mesh elements to propagate by 20%, where the mesh looks less dense than the 1.1 edge growth ratio. The 1.3 edge growth ratio creates even less crowded mesh segments than the 1.2 ratios. The maximum ratio used, which is 1.5, creates mesh segments that are the least crowded, where the mesh propagates gradually over a large distance due to the allowable edge growth ratio, which is 50%. The number of elements and nodes in each mesh differs based on the given ratio. Table 2 shows the mesh growth ratio and the number of elements and nodes for each of the four meshes that have been discussed.

Table 2 - Number of elements and nodes for each mesh edge growth ratio for each horizontal layer

Edge Growth Ratio	1.1	1.2	1.3	1.5
Default Element Size	0.07° = 7.77 km	0.07° = 7.77 km	0.07° = 7.77 km	0.07° = 7.77 km
Number of Elements	132,768	71,630	50,986	35,724
Number of Nodes	69,825	39,256	28,934	21,303

It is worth highlighting that a mesh dependency study was not conducted in this work due to constraints on computational resources. Using a laptop with a 4-core Intel processor and 16 GB of RAM, it took almost five days to complete one simulation (i.e., a model duration equals to 14 days). Hence, the results shown in this paper are intended to be preliminary output based on the methodology presented.

3. Result and Discussion

The results of this study focus on tidal current velocity and tidal kinetic energy flux. Notably, the tidal current velocity obtained was validated against data published by Goh et al. [26]. The limitations of this study and some errors that affect the result of the simulation are also discussed in this section.

3.1 Tidal Current Velocity

The velocity of tidal currents increases between islands with a limited distance or in narrow areas. Fig. 17 and Fig. 18 show the high tide and the low tide for the domain, which are the outcomes of the simulation. The results indicate that tidal velocity accelerates near shorelines due to shallow water conditions as the depth decreases. Additionally, the velocity increases significantly in the southeast part of the domain. This is because the south-eastern part of the domain causes the velocity to increase due to the narrow shape of the domain in that area. The current velocity in the southeast part of the strait accelerates to around 1.1 m/s. This high velocity value could have a high potential for energy extraction because according to Gorbeña et al. [17], energy extraction is economically feasible at a median current velocity higher than 1.1 m/s [4].

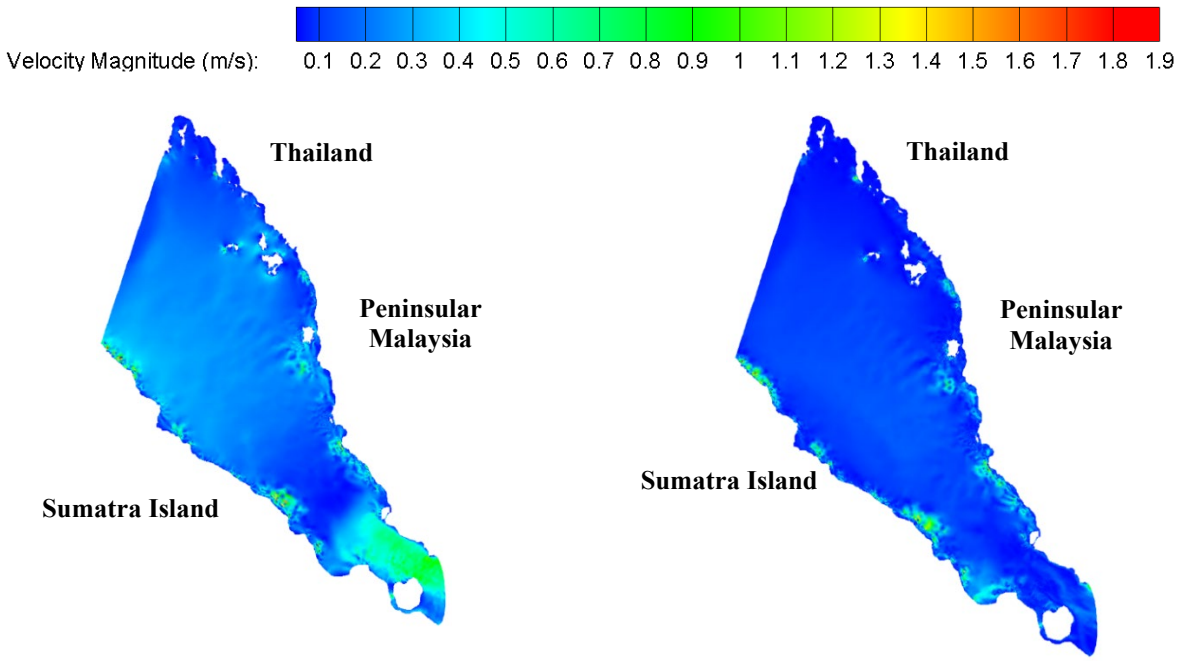

Fig. 17 - Velocity contour showing high tide

Fig. 18 - Velocity contour showing low tide

3.2 Validation

The validation step was conducted by measuring the tidal current velocity of a specific area located on the Malacca Strait and then validated with ADCP current velocity data on the Malacca Strait that was measured by Goh et al. [26]. ADCP (Acoustic Doppler Current Profiler) is a device used to measure the velocity of water across a water column. The device was used to measure the current velocity in the study conducted by Goh et al. [26]. In this study, the validation was conducted by comparing the ADCP tidal current velocity to the simulated tidal current velocity at the same location. As seen in Fig. 19, the ADCP point's coordinates are 2.53059N and 101.74538E, and its location is near Port Dickson.

Fig. 19 - Location of the ADCP point from google maps

Fig. 20 shows two plots that represent the validation of the simulation with the measured data from Goh et al. [26]. The peaks of the lines in the graph represent high tides, while the floors represent low tides. The maximum level reached by the lines represents the spring tide, which can be seen at the beginning and end of the line graph, and the lowest level represents the neap tide, shown at the centre of the graph. The highest velocity is observed on August 2nd, which is approximately 0.97 m/s, whereas it is recorded at a high velocity of 0.70 m/s on July 15th in the simulation data. The lowest velocity in the measured data is slightly below 0 m/s. It is around -0.02 m/s on the 22nd of July. For the simulation data, the lowest velocity is observed on August 7th, which is around 0 m/s. It is worth noting that the data printing period for both the simulation and the observed data is the same, which is 10 minutes.

One thing to note about the validation graph is that the period of the simulation and the measured data were not the same. This means that the period of the spring and neap tides in the simulated data differs from the measured data. Also, the measured data has more peaks than the simulated data, indicating that the high tides recorded in the measured data have a higher velocity than the ones in the simulated data. Significantly, error estimation could not be done in this study because of the following reasons:

a. The simulated result seems to be out of phase with the validation data, and this could be attributed to:
   i. The start date of the simulation model is not the same as the published ADCP data.
   ii. The time step and period of output generation from the model are not synchronised with the measured ADCP data.
b. The reasons stated above happened because details such as the ADCP time step, its data collection interval, and the exact time that the data collection commenced were not stated in the published literature.

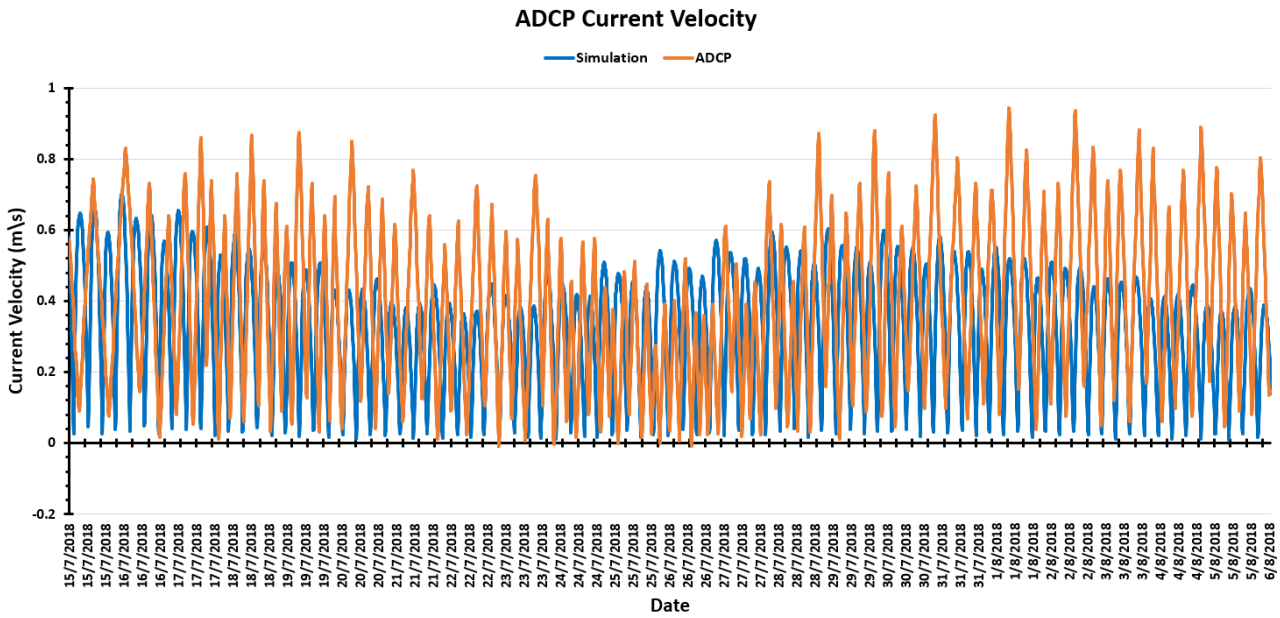

Fig. 20 - Validation of simulated data against published measurement data

3.3 Tidal Energy Flux

Fig. 21 shows the tidal kinetic energy flux for this study, where the temporal details of the energy flux presented are for a period of 12 days. Although the model's simulation period was set for 14 days (refer to Table 1), simulated results from the first two days were omitted to allow the model to reach numerical stability. From this figure, it can be observed that the majority of the high kinetic energy is concentrated in the southeast part of the strait where it narrows down due to the high tidal current velocity in that area, as discussed previously. This high tidal kinetic energy makes the southeast part of the strait a possible location for constructing tidal energy converters. However, more detailed studies should be conducted on the Malacca Strait to see in detail the validity of the southeast part of the strait and to assist in research related to marine renewable energy in Malaysia.

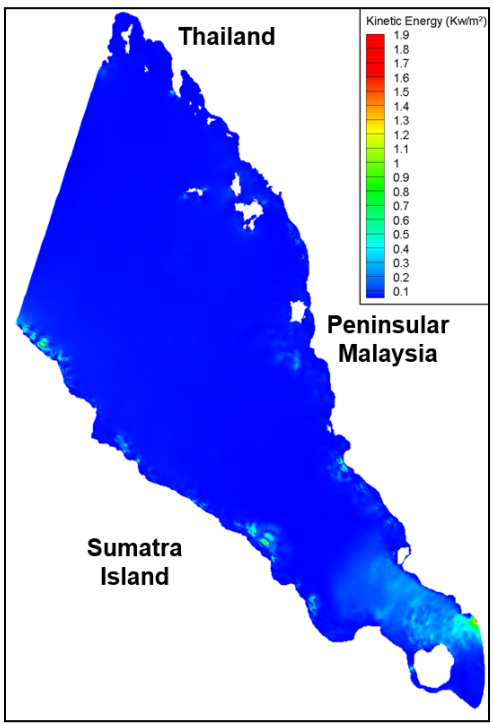

Fig. 21 - Tidal kinetic energy flux of the domain

3.4 Limitations of the Simulation

The results of the simulation performed in this study exhibit a small deviation when compared against the published measurement data. These observed differences could be due to several factors, such as the accuracy of the GEBCO bathymetry data that is freely available to everyone, the open-source coastline data that was extracted from the National Oceanic and Atmospheric Administration (NOAA) webpage, the modifications made to the coastline, and the details of the ADCP measurement data that are not readily available to the public. For instance, the bathymetry data used in this study as well as by Goh et al. [26] was obtained from the same source - the GEBCO website. However, the resolution of the GEBCO data used in this study is 15 arc seconds, whereas the resolution of the data employed by Goh et al. [26] was 30 arcs.

Additionally, the coastline data that was obtained online from the NOAA website was approximate, meaning that it is not identical to the real coastline in the area of interest. Hence, when the model domain was imposed with the TPXO dataset, some inaccuracy was bound to be observed on the imposed domain, which ultimately influenced the outcome of the simulation. Significantly, the modifications made to the coastline via the resampling process as discussed before seemingly to have altered the shape of the coastline. Depending on the values and method used during the resampling process, the shape of the coastline can distinctly vary from the original shape and features. Besides, having too many points on the coastline would add unnecessary load to the computational resources when performing the simulation. Hence, it is important for us to develop a model that has a good balance between numerical accuracy and resource loading. Fig. 22 illustrates the shape of the coastline used in this study compared with the original coastline near Tanjung Tuan headland.

Finally, the depth of the ADCP could also contribute to the differences observed in the validation graph between the measured and simulated data. The depth of the ADCP point in the measured data is 15 m, whereas it is 11 m in the simulated data, and this could be due to the resolution of the GEBCO dataset as previously mentioned. To conclude, all these factors can have a significant influence on the simulation results. Nonetheless, based on the presented results, the model seems to be able to replicate the flow and current characteristics reasonably well. Hence, this research can be used as a reference to provide estimates of the tidal current velocity and kinetic energy flow in the Malacca Strait in future studies.

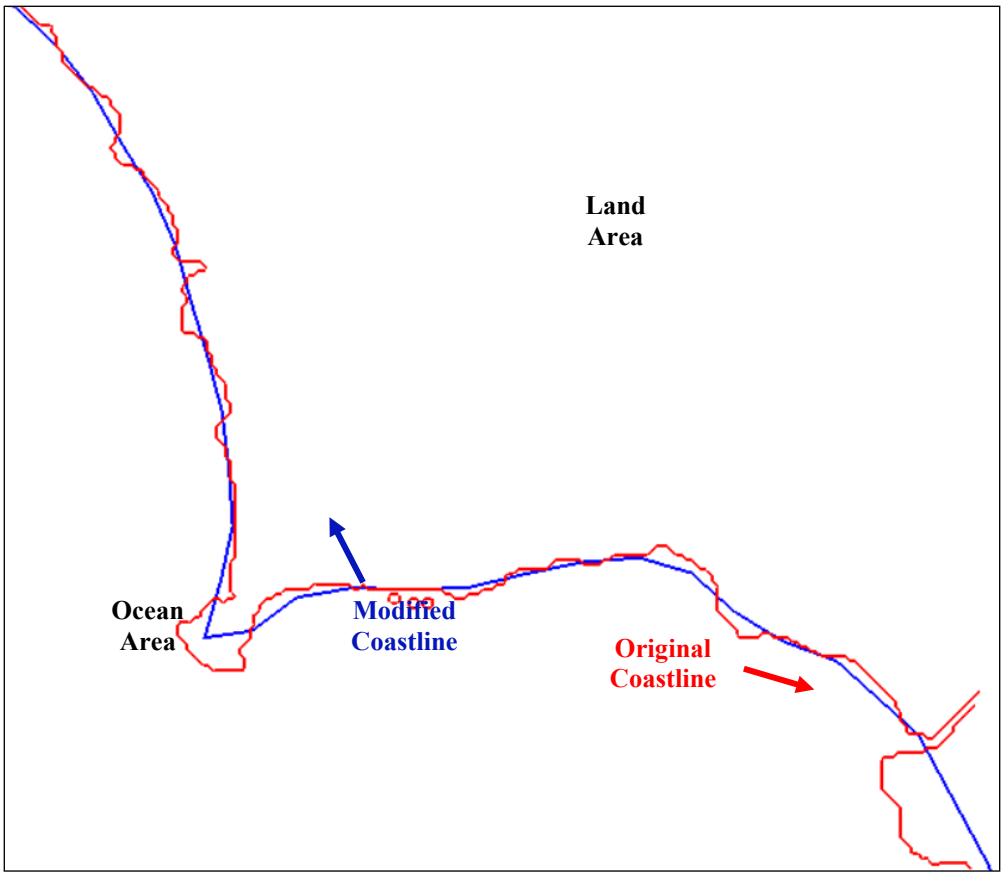

Fig. 22 - The difference between the original coastline and the modified coastline near Tanjung Tuan

4. Conclusion

This study presented a preliminary methodology for developing a three-dimensional flow model for the Strait of Malacca, where some of the issues and complexities involved in setting up an ocean-scale model for this region were highlighted and discussed. The results of high and low tides in the Malacca Strait indicate that the southeast part of the strait has the potential for the installation of tidal energy converters due to the high tidal current velocity activities (up to 1.1 m/s). Significantly, simulation results were validated against the measured ADCP data at a location near Port Dickson. The results demonstrated a high tidal current velocity in the area of up to 0.97 m/s. However, it was observed that the simulated data was out of phase in comparison to the measured data, which can be attributed to several factors, such as the accuracy of the bathymetry and coastline data used in this study. To conclude, this study highlighted that the velocity accelerates around the southeast part of the Malacca Strait, which matched the flow characteristics as observed in past studies. Hence, this implies that the strait has the potential to harness tidal energy from the ocean to power the Malaysian grid.

Acknowledgement

The authors gratefully acknowledge the support received from the Ministry of Higher Education Malaysia through the Fundamental Research Grant Scheme for Research Acculturation of Early Career Researchers (FRGSRACER) RACER/1/2019/TK07/UNIMAP/1. Additionally, the authors are also thankful for the support given by Universiti Malaysia Perlis, specifically from the Research Management Centre (RMC).

References

[1] Energy Commission of Malaysia, *Malaysia Energy Statistics Handbook*. Putrajaya, 2020.

[2] H. N. Afrouzi, H. P. Pvs, H. Sundram, T. S. Kieh, K. Mehranzamir, and C. L. Wooi, "Review on Feasibility of Gravity Power Generation Mechanism in Malaysia's Sustainable Energy Program," *Int. J. Integr. Eng.*, vol. 13, no. 2, pp. 109 -118, 2021, doi: 10.30880/ijie.2021.13.02.013.

[3] K. W. Tan, B. Kirke, and M. Anyi, "Small-scale hydrokinetic turbines for remote community electrification," *Energy Sustain. Dev.*, vol. 63, pp. 41 -50, 2021, doi: 10.1016/j.esd.2021.05.005.

[4] F. Ghazali and M. Mustafa, "Marine renewable energy legal framework in Malaysia: A way forward," *J. Sustain. Sci. Manag.*, vol. 15, no. 3, pp. 101 -112, 2020.

[5] X. L. Khai *et al.*, "Harvesting Electrical Energy from Rooftop Ventilator," *Int. J. Integr. Eng.*, vol. 10, no. 4, pp. 68 -72, 2018, doi: 10.30880/ijie.2018.10.04.011.

[6] Z. H. Bohari, M. F. Baharom, M. H. Jali, M. F. Sulaima, and W. M. Bukhari, "Are tidal power generation suitable as the future generation for Malaysian climate and location: A technical review?," *Int. J. Appl. Eng. Res.*, vol. 11, no. 10, pp. 7095 -7099, 2016.

[7] N. R. Maldar, C. Y. Ng, M. S. Patel, and E. Oguz, "Potential and prospects of hydrokinetic energy in Malaysia: A review," *Sustain. Energy Technol. Assessments*, vol. 52, no. PC, p. 102265, 2022, doi: 10.1016/j.seta.2022.102265.

[8] M. Hossain *et al.*, "A state-of-the-art review of hydropower in Malaysia as renewable energy: Current status and future prospects," *Energy Strateg. Rev.*, vol. 22, no. July 2017, pp. 426 -437, 2018, doi: 10.1016/j.esr.2018.11.001.

[9] X. Liu *et al.*., "A review of tidal current energy resource assessment in China," *Renew. Sustain. Energy Rev.*, vol. 145, no. March, 2021, doi: 10.1016/j.rser.2021.111012.

[10] H. Y. Chong and W. H. Lam, "Ocean renewable energy in Malaysia: The potential of the Straits of Malacca," *Renew. Sustain. Energy Rev.*, vol. 23, pp. 169 -178, 2013, doi: 10.1016/j.rser.2013.02.021.

[11] H. B. Goh, S. H. Lai, M. Jameel, and H. M. Teh, "Potential of coastal headlands for tidal energy extraction and the resulting environmental effects along Negeri Sembilan coastlines: A numerical simulation study," *Energy*, vol. 192, p. 116656, 2020, doi: 10.1016/j.energy.2019.116656.

[12] P. A. J. Bonar, A. M. Schnabl, W. K. Lee, and T. A. A. Adcock, "Assessment of the Malaysian tidal stream energy resource using an upper bound approach," *J. Ocean Eng. Mar. Energy*, 2018, doi: 10.1007/s40722-018-0110-5.

[13] A. S. Sakmani, W. H. Lam, R. Hashim, and H. Y. Chong, "Site selection for tidal turbine installation in the Strait of Malacca," *Renew. Sustain. Energy Rev.*, vol. 21, pp. 590 -602, 2013, doi: 10.1016/j.rser.2012.12.050.

[14] V. M. Aboobacker, "Wave energy resource assessment for eastern Bay of Bengal and Malacca Strait," *Renew. Energy*, 2017, doi: 10.1016/j.renene.2016.09.016.

[15] C. B. Jiang *et al.*, "High-resolution numerical survey of potential sites for tidal energy extraction along coastline of China under sea-level-rise condition," *Ocean Eng.*, vol. 236, no. March, 2021, doi: 10.1016/j.oceaneng.2021.109492.

[16] M. R. Hashemi and S. P. Neill, "The role of tides in shelf-scale simulations of the wave energy resource," *Renew. Energy*, 2014, doi: 10.1016/j.renene.2014.03.052.

[17] A. Rahman and V. Venugopal, "Parametric analysis of three dimensional flow models applied to tidal energy sites in Scotland," *Estuar. Coast. Shelf Sci.*, vol. 189, pp. 17 -32, 2017, doi: 10.1016/j.ecss.2017.02.027.
[18] NOAA, "NOAA Tides & Currents," 2021. https://toolkit.climate.gov/tool/noaa-tides-currents (accessed Jun. 01, 2022).
[19] Y. S. Lim and S. L. Koh, "Analytical assessments on the potential of harnessing tidal currents for electricity generation in Malaysia," *Renew. Energy*, vol. 35, no. 5, pp. 1024 -1032, 2010, doi: 10.1016/j.renene.2009.10.016.
[20] M. J. Suárez-López, R. Espina-Valdés, V. M. F. Pacheco, A. N. Manso, E. Blanco-Marigorta, and E. Álvarez-Álvarez, "A review of software tools to study the energetic potential of tidal currents," *Energies*, vol. 12, no. 9, 2019, doi: 10.3390/en12091673.
[21] K. S. Lee and L. Y. Seng, "Preliminary investigation of the potential of harnessing tidal energy for electricity generation in Malaysia," 2008. doi: 10.1109/TDC.2008.4517098.
[22] K. S. Lee and L. Y. Seng, "Simulation Studies on the Electrical Power Potential Harnessed by Tidal Current Turbines," *J. Energy Environ.*, vol. 1, pp. 18 -23, 2009.
[23] H. Y. Chong and W. H. Lam, "Ocean renewable energy in Malaysia: The potential of the Straits of Malacca," *Renew. Sustain. Energy Rev.*, vol. 23, pp. 169 -178, 2013, doi: 10.1016/j.rser.2013.02.021.
[24] M. Mahgoub, R. Hinkelmann, and M. La Rocca, "Three-dimensional non-hydrostatic simulation of gravity currents using TELEMAC3D and comparison of results to experimental data," *Prog. Comput. Fluid Dyn.*, vol. 15, no. 1, pp. 56 -67, 2015, doi: 10.1504/PCFD.2015.067325.
[25] EDF, "TELEMAC-3D Software Release 7.0 REFERENCE MANUAL," 2015. http://wiki.opentelemac.org/doku.php?id=user_manual_telemac-3d
[26] H. B. Goh, S. H. Lai, M. Jameel, H. M. Teh, and R. J. Chin, "Feasibility assessment of tidal energy extraction at the Tg Tuan coastal headland: A numerical simulation study," *Sustain. Energy Technol. Assessments*, vol. 38, no. December 2019, p. 100633, 2020, doi: 10.1016/j.seta.2020.100633.